

# MHD modeling and optimization of a passive helical coil for mitigation of runaway electrons

D.B. Weisberg<sup>1\*</sup>, C. Paz-Soldan<sup>1,2</sup>, Y.Q. Liu<sup>1</sup>, A. Battey<sup>2</sup>, A. Welander<sup>1</sup>, C. Murphy<sup>1</sup>, C. Crowe<sup>1</sup>, C. Dunn<sup>3</sup>

<sup>1</sup>General Atomics, <sup>2</sup>Columbia University, <sup>3</sup>Georgia Tech.

\*weisbergd@fusion.gat.com



## ABSTRACT

- Numerical modeling of a helical coil designed to passively generate non-axisymmetric fields during a plasma disruption shows efficient deconfinement of runaway electrons (RE)<sup>1</sup>.
- Optimization of coil geometry is performed using TokSys<sup>2</sup> electromagnetic analysis of inductive coupling during current quench (CQ), and SURFMN<sup>3</sup> vacuum island overlap width (VIOW) generated in experimental equilibria.
- Relativistic drift orbit tracing using the linear MHD code MARS-F<sup>4,5</sup> predicts up to 70% of RE orbits lost after 200 $\mu$ s.

## BACKGROUND

- Previous studies<sup>6</sup> have demonstrated the feasibility of RE deconfinement via the application of 3D fields.
- A proposed in-vessel helical coil would inductively couple to the disruption current quench and generate a large 3D field to limit RE formation. Ideal tokamak models have defined thresholds for coil current and field<sup>7</sup>:

$$\frac{I_{coil}}{I_P} \gtrsim 2\%, \quad \frac{\delta B}{B_0} \gtrsim 10^{-2}$$

- This study investigates the parametric optimization of an in-vessel helical coil as a passive safety measure against RE beam formation.
  - What is the optimal coil geometry to maximize RE orbit loss?
  - How would an RE coil design installed and validated on DIII-D scale to reactor-relevant devices?

## MODELING RESULTS

Inductive coupling modeling shows that the induced coil current can be as large as 12% of the pre-disruption plasma current (Fig. 3).

- Adding an outboard poloidal loop decreases this by up to a factor of 2
- Induced current is highest for shallow helical angle (low  $Z_{CP}$ ), which minimizes the average distance between the coil and the plasma

Vacuum field modeling shows that  $\delta B$  can be as large as 1% of equilibrium toroidal field, and that an optimized coil will generate VIOW of up to 0.7  $\Psi_N$ .

- VIOW increases discontinuously with coil current as  $n=1$  and  $n=2$  vacuum islands grow large enough to overlap each other (Fig. 4)
- The VIOW-optimized parameter space is broad, allowing a single coil shape to efficiently couple to resonant plasma modes in both test equilibria (Fig. 5)

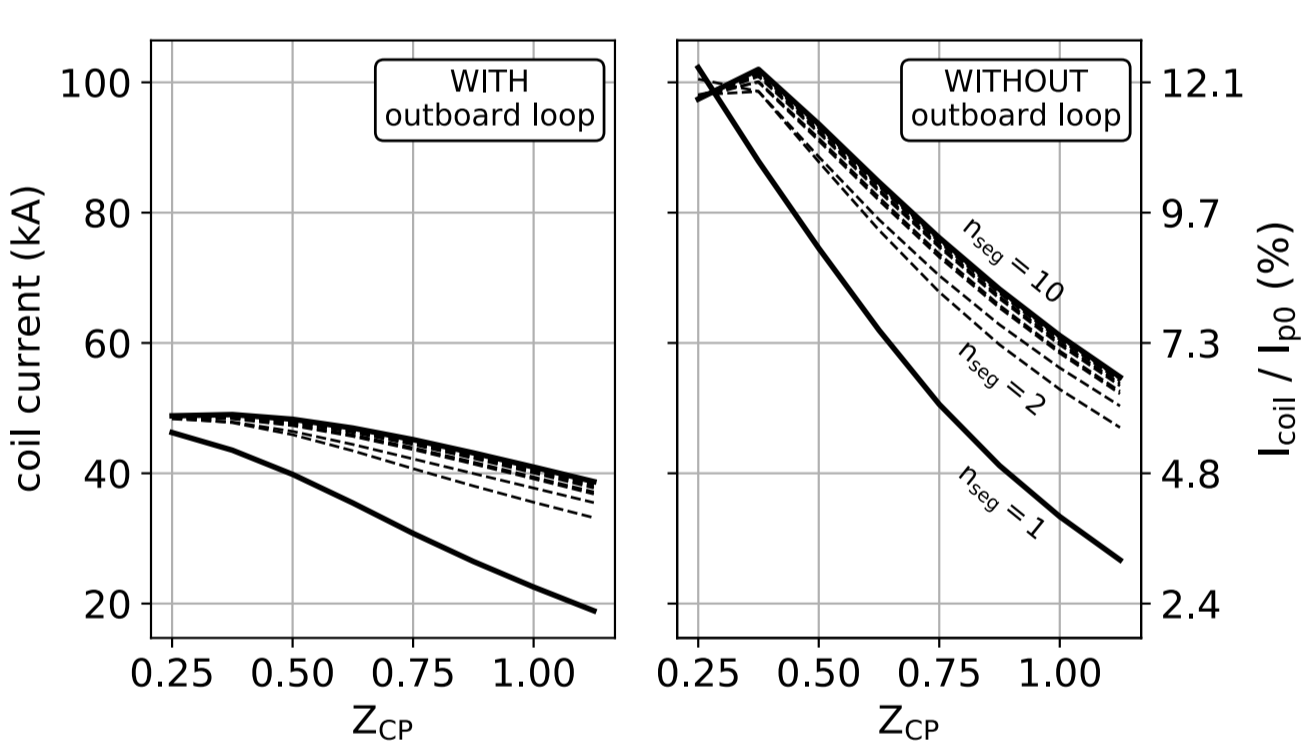


Fig 3. Induced current ( $t = 6ms$ )

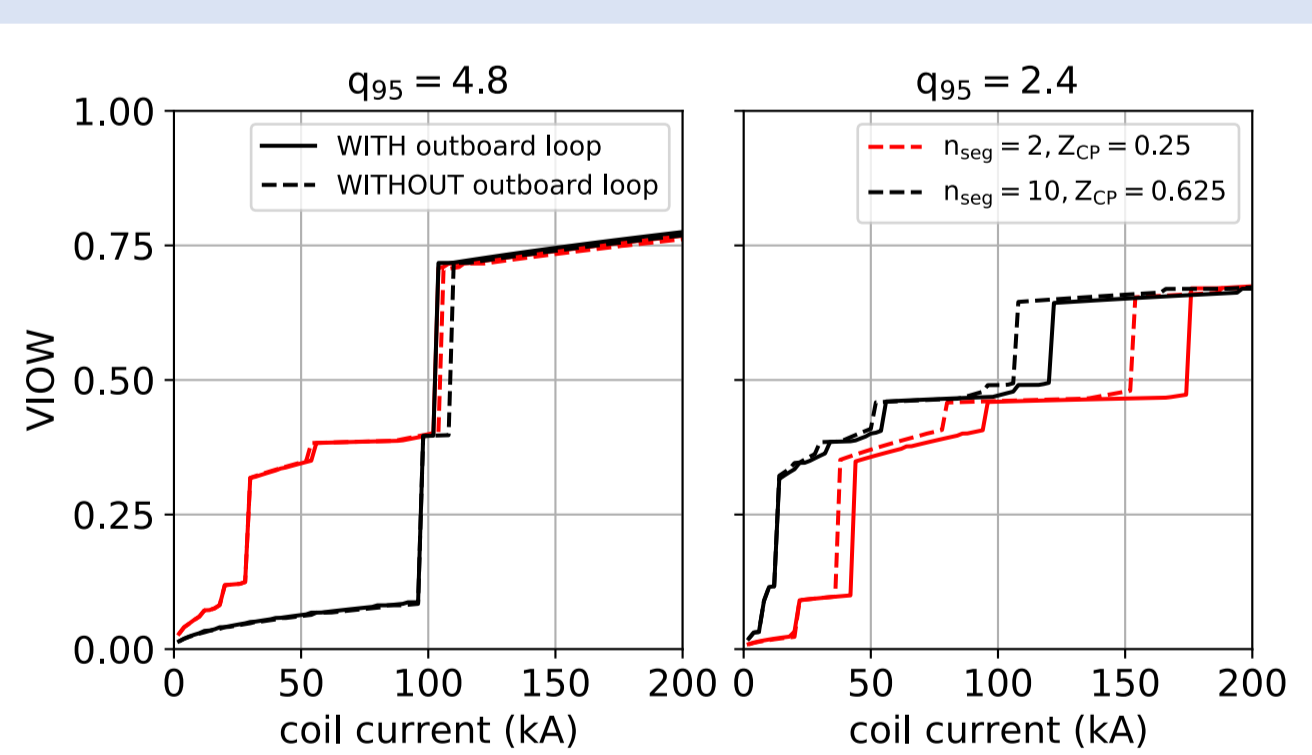


Fig 4. VIOW vs. coil current for Mk1 & Mk2 coils

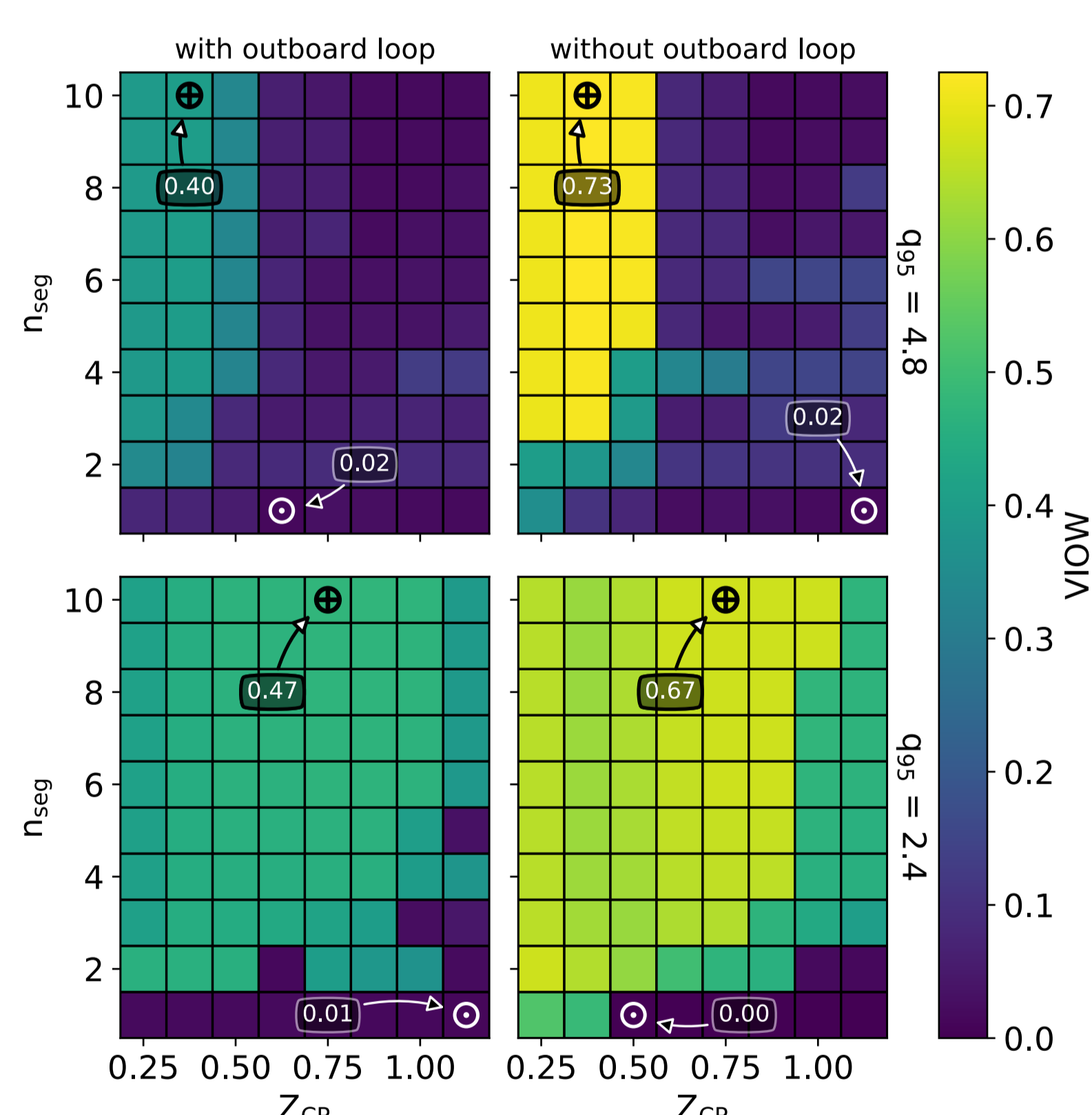


Fig 5. Induced VIOW over coil geometry scan, for both test equilibria

## CONCEPTUAL DESIGN

Engineering modeling has converged on a conceptual design for an RE coil for installation on the DIII-D tokamak. Modifications are made to account for:

- Available conductor path along DIII-D vacuum vessel wall
- Addition of leads to port feed-thru and ex-vessel switch
- Detailed design of structural attachment to vessel wall

Finite-element analysis shows coil stress and deformation are well within material limits (Fig. 8).

- Conductor is CuCrZr, with mica insulator

Psi-Tet 3D modeling shows time-delay caused by mirror currents in vacuum vessel (Fig. 9).

- Increased coil-wall stand-off results in higher field, but does not change time delay

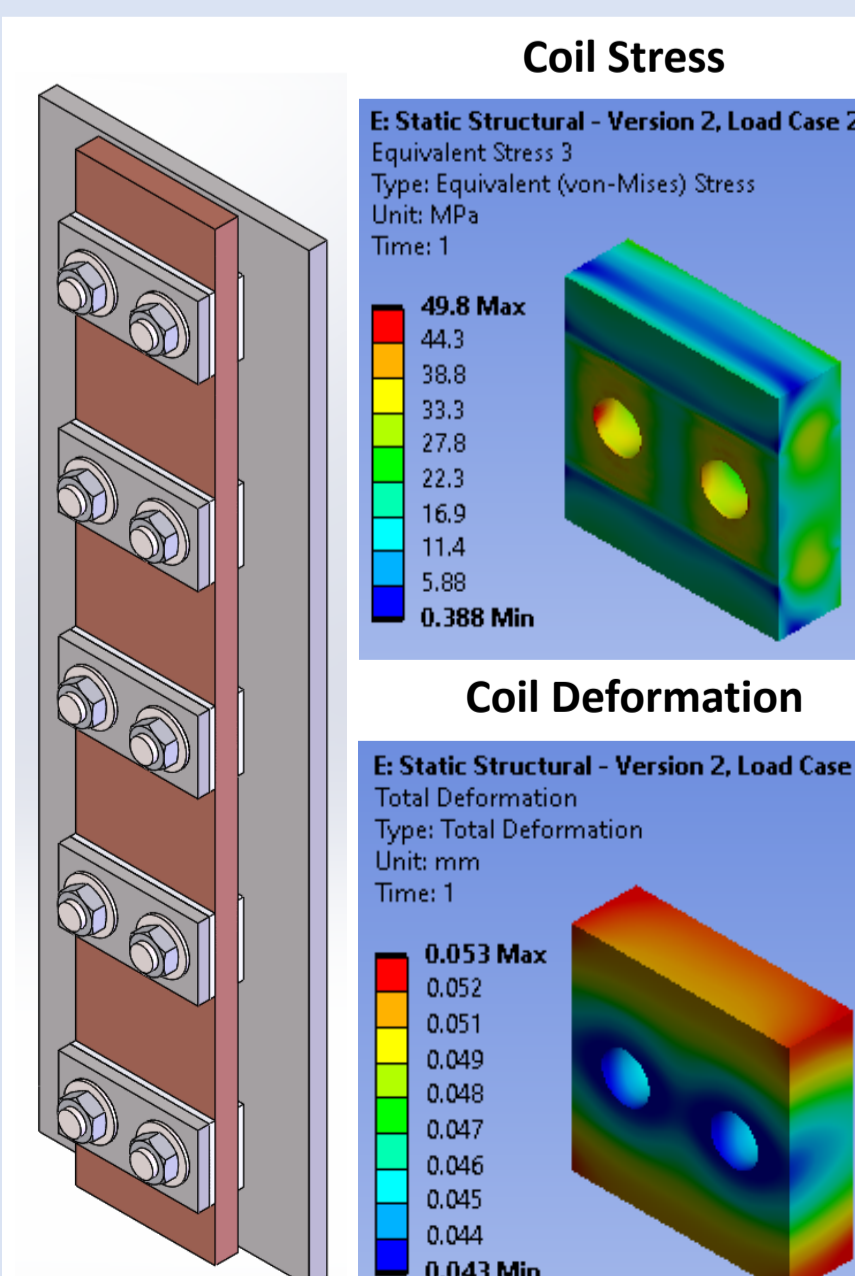
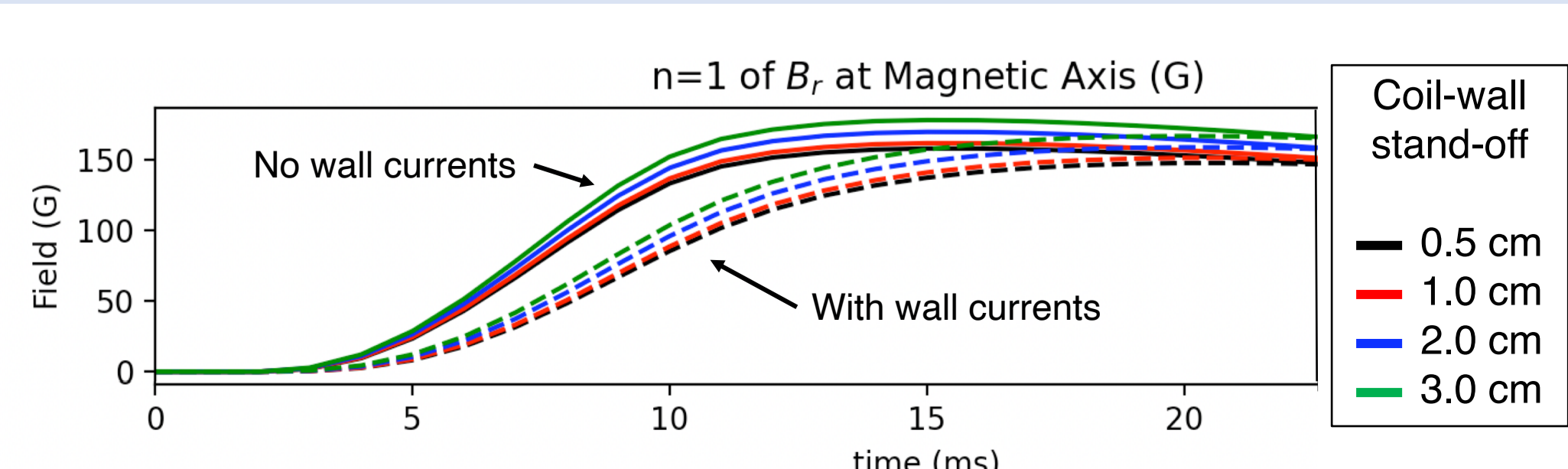


Fig 8. ANSYS structural modeling for RE coil operation

Fig 9. Psi-Tet electromagnetic modeling shows effect of 3D vacuum vessel eddy currents

## OPTIMIZATION WORKFLOW

### I. COIL PARAMETRIZATION

The helical coil geometry is defined by three parameters (Fig. 1):

- Pitch angle of centerpost helix ( $Z_{CP}$  = height of  $n=1$  helix)
- Discrete number of vertical helix segments ( $n_{seg}$ )
- Absence or presence of poloidal outboard loop

### II. VACUUM FIELD OPTIMIZATION

TokSys and SURFMN are used to calculate the vacuum island overlap width (VIOW) metric over a range of coil geometries. Two mid-CQ equilibria from RE-producing experiments on DIII-D are used as test cases (Fig. 2), with high- $I_P$  ( $q_{95}=2.4$ ) and low- $I_P$  ( $q_{95}=4.8$ ).

### III. RELATIVISTIC DRIFT ORBIT TRACING

Based on the vacuum field results, several coil geometries are selected for analysis in MARS-F. The full plasma response is calculated, and the orbits of an initial distribution of relativistic test particles are traced. The loss fraction of RE orbits is compared between coil geometries and equilibria.

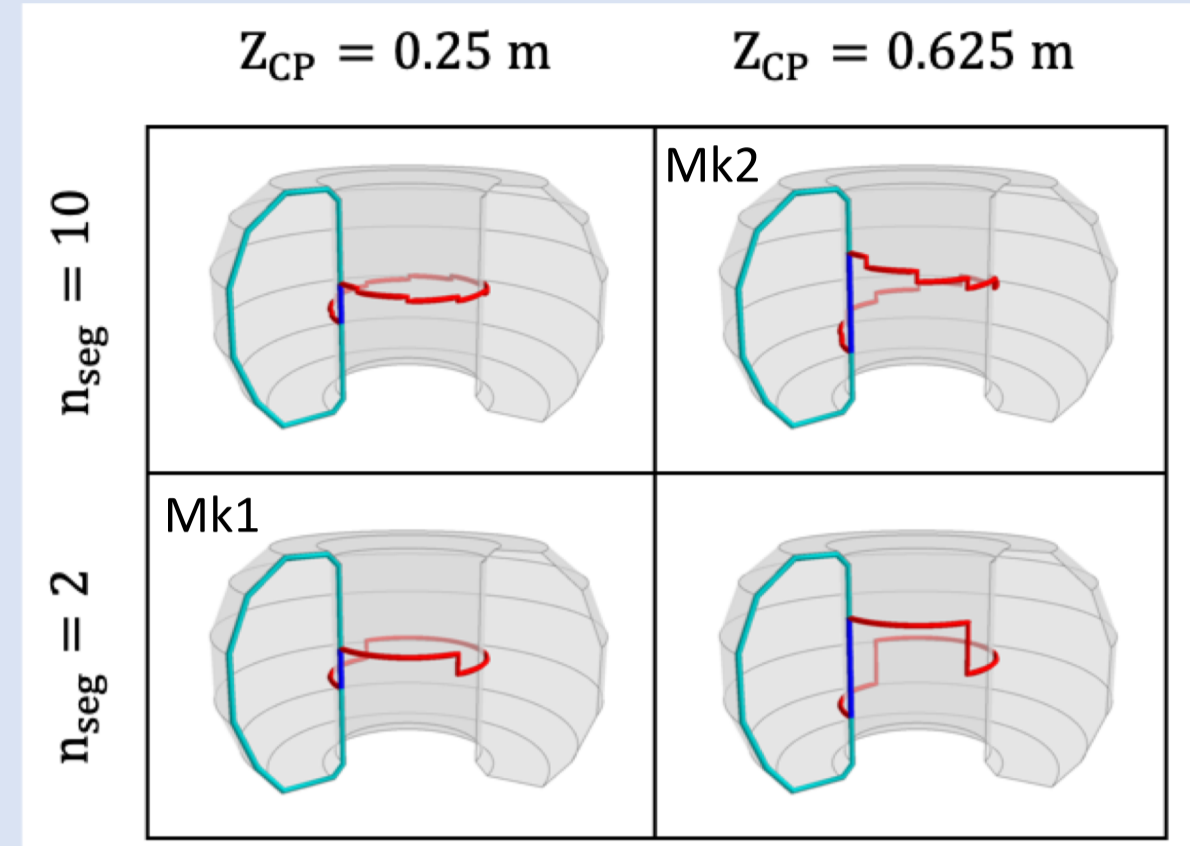


Fig 1. Coil geometry parametrization

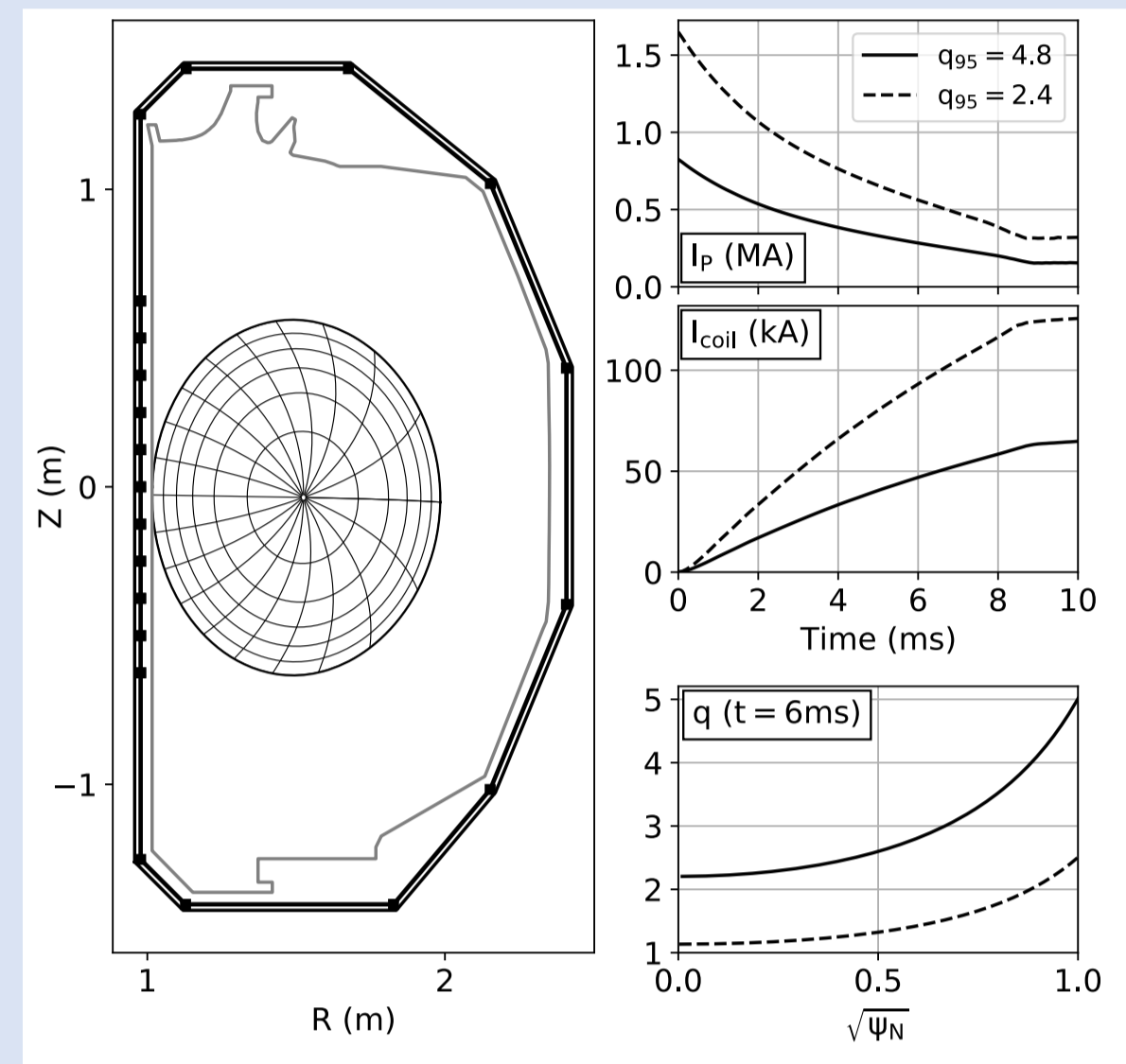


Fig 2. DIII-D equilibria and current evolution

Drift orbit tracing shows that up to 70% of RE orbits are lost within 200 $\mu$ s, with increased loss fraction observed at higher coil current and plasma current.

- Two coil shapes were chosen for MARS-F modeling: Mk1 and Mk2 (see Fig. 1)
- Mk2 design outperforms Mk1 in all cases, although for low- $I_P$  there is a delay in the orbit loss fraction (Fig. 6)

Further analysis of outboard RE orbits reveals evidence of RE trapping between  $q=3/1$  and  $q=4/1$  island chains in low- $I_P$  equilibrium (Fig. 7).

- Larger islands formed by 100kA Mk2 coil decrease outboard-born RE orbit loss fraction via resonant trapping; explains 2-step evolution of orbit loss
- This phenomenon is not observed at high- $I_P$ , which has fewer  $n=1$  surfaces

Non-linear MHD modeling<sup>8</sup> confirms these results and shows that RE loss will be measurable in DIII-D experiments. See Izzo contributed talk on Thursday afternoon for more details.

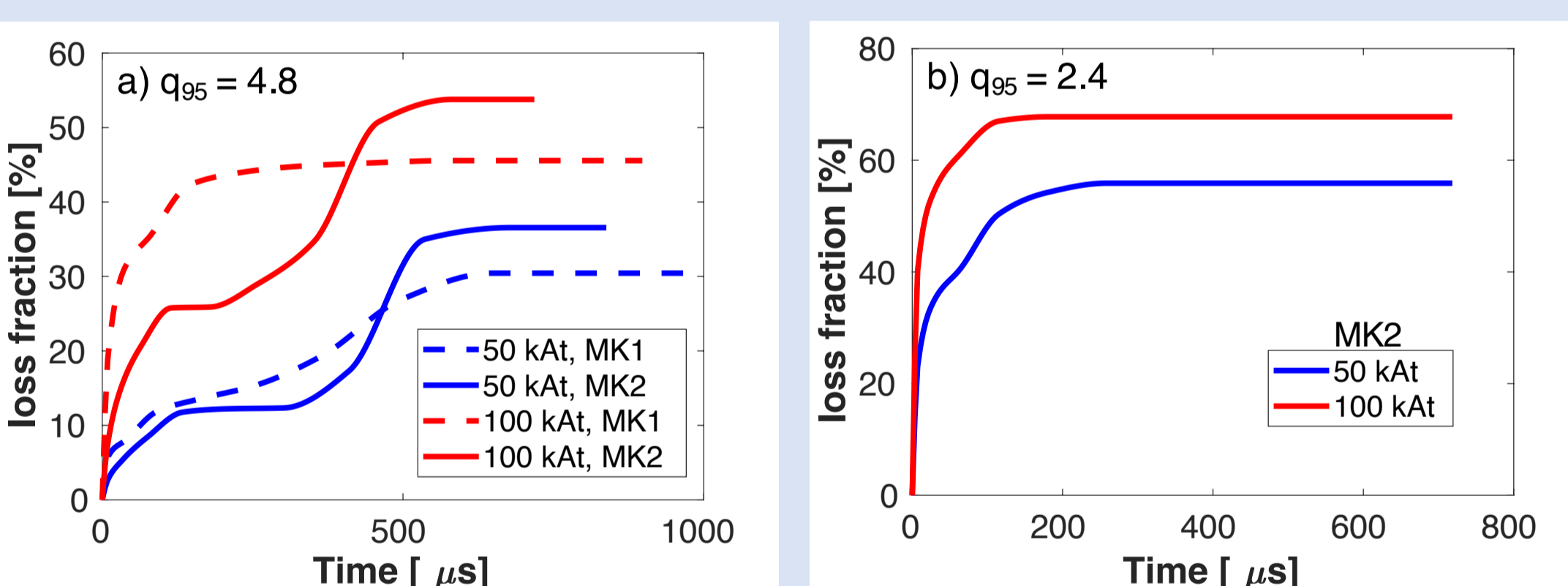


Fig 6. RE orbit loss fraction for a) low- $I_P$ , b) high- $I_P$  cases

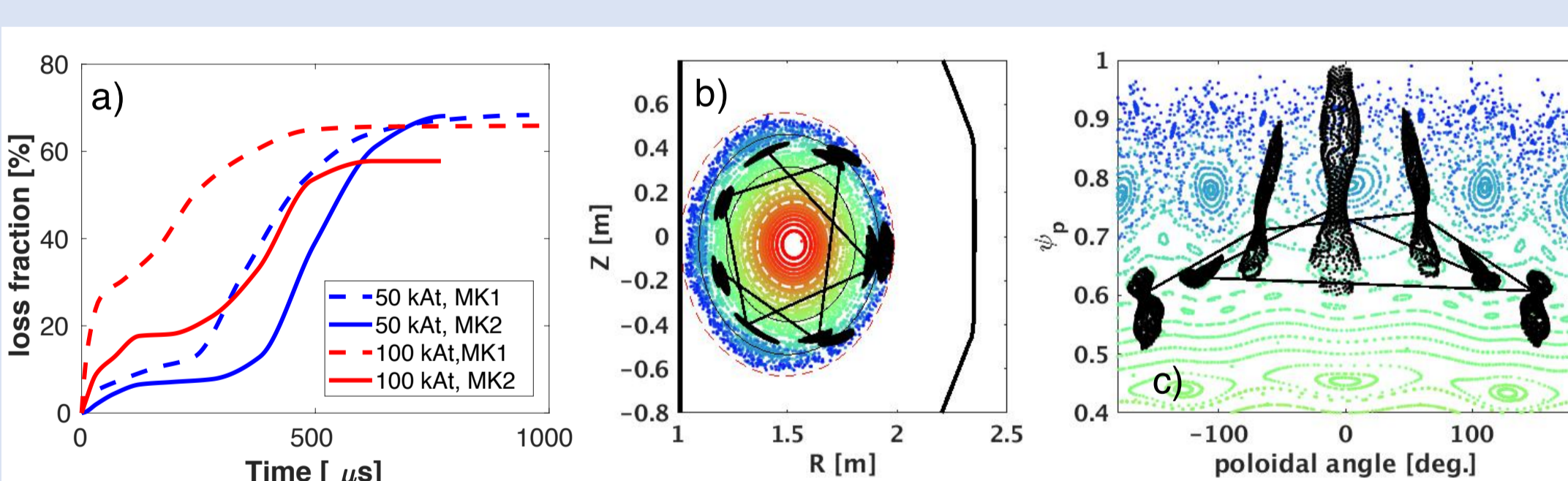


Fig 7. RE orbit-trapping in low- $I_P$  case: a) outboard-born RE loss evolution, b,c) RE orbit for 100kA Mk2 for  $0 < t < 283\mu s$ .

Param	Scale factor	ITER-like
$I_P$	$M_I$	7.5
$B_T$	$M_B$	2.0
$R_0$	$M_R$	3.75
$N$	$M_N$	1
$q_{95}$	$M_R M_B / M_I$	1
$\tau_{CQ}$	$M_R^2$	14
$I_{coil} / I_P$	$M_i / M_I$	1
$\delta B / B_T$	$M_N M_B / M_B$	1
$F_{J \times B}$	$M_i^2 / M_R$	15
$\sigma_{J \times B}$	$M_N M_i^2 / M_R^3$	1.07
$P_{Joule}$	$M_R^2 M_i^2 / M_R$	210
$\Delta T_{coil}$	$M_N^2 M_i^2$	56

Table 1. Stress and thermal scale factors

## CONCLUSIONS

Vacuum field optimization of RE mitigation coil geometry shows a broad minimum in parameter space, and drift orbit tracing of two specific coil shapes shows efficient RE loss for multiple plasma equilibria.

- $I_{coil} / I_P$  and  $\delta B / B_T$  are scale-independent (at constant aspect ratio and  $q_{95}$ ), so an experimentally validated DIII-D coil design will be equally efficient on larger, higher-current reactor-relevant tokamaks.

- Structural and thermal stresses are not scale-independent, but are still manageable on an ITER-size device (Table 1). Notably, while  $\Delta T_{coil}$  increases by a factor of 56 from DIII-D to ITER scales,  $\Delta T_{DIII-D} \sim 2^\circ C$  and so  $\Delta T_{ITER} \sim 100^\circ C$ .

Non-linear MHD modeling (NIMROD) has shown the above confinement results to be conservative, with the prediction of near-complete RE loss in typical DIII-D experimental cases.

## ACKNOWLEDGEMENTS / REFERENCES

This material is based upon work supported by the U.S. Department of Energy, Office of Science, Office of Fusion Energy Sciences, using the DIII-D National Fusion Facility, a DOE Office of Science user facility, under Award(s) DE-FC02-04ER54698, as well as by internal General Atomics funds.

- Weisberg, D et al., *Nucl. Fusion* **61** (2021) 106033.
- Humphreys, D et al., *Nucl. Fusion* **47** (2007) 943-951.
- Schaffer, M et al., *Nucl. Fusion* **48** (2008) 024004.
- Liu, YQ et al., *Phys. Plasmas* **7** (2000) 3681-3690.
- Liu, YQ et al., *Nucl. Fusion* **59** (2019) 126021.
- Smith, HM et al., *Phys. Plasmas* **20** (2013) 072505.
- Boozer, A, *PPCF* **53** (2011) 084002.
- Izzo, V et al., *in review*